Curves of Growth of Autoionizing Spectral Lines with Application to the 3s-4p Transition in Argon*

Ara Chutjian

Department of Chemistry, University of Southern California
Los Angeles, California 90007

and

Jet Propulsion Laboratory, California Institute of Technology
Pasadena, California 91103†

and

Robert W. Carlson

Department of Physics, University of Southern California
Los Angeles, California 90007

*This work was supported by the National Science Foundation (GP-5294) and the National Aeronautics and Space Administration (NGR-05-018-065 and NGL-05-018-044), and also in part by the National Aeronautics and Space Administration under Contract No. NAS7-100. A preliminary report was given at the 1969 West Meeting of the American Physical Society (Bull. Am. Phys. Soc. 14, 1180 (1969). (Submitted for publication to the Journal of Optical Society, March 1970)

†Present address.

ABSTRACT

Curves of growth are calculated for autoionizing transitions having the Beutler-Fano form of absorption cross section. Both graphs and tabulated values of the curves are presented. The curve-of-growth analysis is applied to the 3s-4p transition in argon at λ 466 Å. The line parameters Γ, q, and ρ^2 obtained by fitting the theoretical and experimental equivalent widths are in good agreement with other high-resolution values. The curve-of-growth technique thus appears to be an attractive method for determining the parameters of autoionizing features. The application of this technique to making path length or particle density measurements in, for example, a King furnace or a plasma is also discussed.

INTRODUCTION

Thanks to the development of strong light sources and good detectors for the vacuum ultraviolet region, there has been much recent interest in the measurements of intensities of autoionizing line profiles. The theoretical work of Fano[1] and Fano and Cooper[2] has led to a characterization of the autoionizing lines first seen by Beutler[3] in the rare gases. Several recent experimental measurements have confirmed the theoretical interpretation of the line shapes, and have led to accurate values of the relevant line parameters. Among these are the photographic measurements of Madden and Codling[4] on the $2s2p\ ^1P^o$ state of helium, and the photoelectric and photographic measurements of Levy and Huffman[5] and Madden, Ederer, and Codling[6] on the 3s-4p Rydberg member in argon.

In the present work we will explore the curve-of-growth technique[7] to characterize the shape and width of autoionizing line profiles. Just as with the more conventional Lorentzian, Doppler, or Voigt profiles, the approach here is useful for extracting line parameters, or making pressure or path-length measurements, in cases where the autoionizing line-width is comparable to, or several times smaller than, the slitwidth of the spectrometer used in the measurements. This predicament arises when we are confined to the use of weak light sources, or when the width of the autoionizing level itself is small as in, say, the helium $(sp, 23+)\ ^1P^o$ state.[4]

We will present the curves of growth for lines having the Beutler-Fano form of the absorption cross section. We will also apply the technique to the 3s-4p transition in argon. In this way we will both illustrate the curve-of-growth method, and give some idea as to the accuracy to which one can measure

the line parameters.

THEORETICAL CONSIDERATIONS

Following the treatment of Fano and Cooper[2] we represent the absorption cross section in the vicinity of an autoionizing transition as

$$\sigma(\epsilon)(\mathrm{cm}^2) = \sigma_a[(q+\epsilon)^2/(1+\epsilon^2)] + \sigma_b \ . \qquad (1)$$

Here $\epsilon = (\omega-\omega_0)/(\frac{1}{2}\Gamma)$ is the distance from the resonance (centered at ω_0) in units of $\frac{1}{2}\Gamma$, ω is the energy of the incident photon, and Γ is $\hbar$ divided by the lifetime of the autoionizing state. The parameter q^2 is the matrix element which connects the lower state and the "modified" discrete state[1], divided by the matrix element which connects the lower state and a bandwidth Γ of continuum states which interact with the discrete state. The quantity σ_a is the absorption cross section to the continuum which mixes with the discrete state, while σ_b is the absorption cross section to any other continua which do not interact with the discrete state.

We can rewrite Eq. (1) as

$$\sigma(\epsilon) = \sigma_t[1 + \rho^2(q^2-1+2q\epsilon)/(1+\epsilon^2)] \ , \qquad (2)$$

where $\sigma_t = \sigma_a + \sigma_b$ is the total absorption cross section away ($\epsilon \gg 1$) from the resonance, and ρ^2 is the ratio σ_a/σ_t. We define the equivalent width as the net area of the autoionizing feature (relative to the baseline determined by σ_t) divided by the incident light intensity. If we let I_0 be the incident light intensity, then the transmitted intensity I in the presence of the

continua is $I = I_0 \exp(-\sigma_t N\ell)$ where N is the number of lower state atoms or molecules per cm^3, and ℓ the absorption path length in cm. The equivalent width is then (in units of eV, for example)

$$W(eV) = \int_{-\infty}^{\infty} \frac{I_0 \exp[-\sigma_t N\ell] - I_0 \exp[-\sigma(\epsilon)N\ell]}{I_0} \, d\omega(eV) \, . \tag{3}$$

Using Eq. (2), and after several straightforward manipulations, we can transform Eq. (3) into the easy-to-use form

$$\frac{W(q,\rho^2,\beta)}{\Gamma} = \exp[\beta(\rho^2-1)] \left\{ \exp(-\rho^2\beta) \times \right.$$
$$\left. \times \int_0^{\infty} \left[1 - \exp\left(-\rho^2\beta \, \frac{q^2-1}{1+\epsilon^2}\right) \cosh\left(\rho^2\beta \, \frac{2q\epsilon}{1+\epsilon^2}\right) \right] d\epsilon \right\} , \tag{4}$$

where the left-hand side is now $W(q,\rho^2,\beta)/\Gamma$ and where $\beta = N\sigma_t\ell$ is a measure of the strength of the absorption, and is an experimentally obtainable quantity.

There are several interesting features to Eq. (4). All the variables $(W/\Gamma, q, \rho^2, \beta, \epsilon)$ are dimensionless, so that Eq. (4) and the subsequent curves of growth are quite universal, and apply to all experimental setups. Also, from the way we have split up the first two exponential factors, we have the following generating equation

$$\frac{W(q,\rho^2,\beta)}{\Gamma} = \exp[\beta(\rho^2-1)] \, \frac{W(q,1,\rho^2\beta)}{\Gamma} \, . \tag{5}$$

This equation eliminates ρ^2 as an independent parameter in the calculation of the curves of growth. We can now calculate a set of curves of growth for different q, and with $\rho^2 = 1$. We then have the set of curves for any other $\rho^2 < 1$ from Eq. (5).

Finally, we note that W/Γ is an even function in q. This means that formally we can only get the magnitude of q from a curve-of-growth analysis. But in practice, if the finite resolution of the spectrometer has not distorted the line shape too badly, then one can often determine the sign of q by looking for the asymmetry in the experimentally-broadened line shape (see Fig. 2). In many cases, however, the sign of q may not be needed, since important physical quantities, such as the absorption f-value to the modified discrete state, depend on q^2.

We could find no closed form expression for the integral in Eq. (4), so we evaluated it numerically by the method of Gaussian quadratures.[8] The value of the integral $W(q,1,\beta)/\Gamma$ was calculated in 0.25 and 0.50 steps in β for $0 \leq \beta \leq 8$; and in 0.5 steps in q for $0 \leq q \leq 3$. We found that for an upper limit to the integration of $\epsilon = \epsilon_{max} = 10^4$, the relative error in the truncation from ϵ_{max} to ∞ was always less than 0.035%. The relative error in the convergence of the integral was held to less than 0.015%, or roughly to one-half the truncation error. The slow convergence of the integral stems from the fact that the integrand in Eq. (4) goes as $1/\epsilon^2$ for large ϵ (where $1 + \epsilon^2 \sim \epsilon^2$, and where the exponential and hyperbolic cosine expansions are appropriate), so that the truncation error is proportional to $1/\epsilon_{max}$.

The computed values of $W(q,1,\beta)/\Gamma$ are presented in Table I, and in graphical form in Fig. 1. The values can be easily interpolated in β. Where the curve of growth for a non-tabulated value of q is desired, it may be interpolated from the values in Table I. This procedure will be accurate to about 1-5%, and it may not be necessary in some cases to evaluate Eq. (4) numerically for the intermediate value of q.

It is interesting to note that the equivalent widths in Table I and Fig. 1 are negative for most β and for most q. This is in contrast to the usual curves of growth[7] where the equivalent width is always positive, and is a reflection of the fact that the autoionizing feature, for most q and β, is a relative <u>emission</u> feature. (As can be seen in Fig. 2, the feature stands out above its background given by $I/I_0 = \exp(-\sigma_t N\ell)$.) At the point $\epsilon = -q$ in Eq. (1) the cross section has a relative minimum and gives rise to a "transmission window." Mathematically, the hyperbolic cosine factor in Eq. (4) is increasing rapidly with ϵ for most values of q and β, so that the integrand is usually negative.

EXPERIMENTAL DETAILS

We were able to measure the variation of W with β for the 3s-4p Rydberg transition in argon, and to compare these results with the curve of growth calculated from Eq. (4), using the line parameters from the high-resolution measurements of Madden, Ederer, and Codling.[6]

The experimental apparatus consisted of the following elements: a pulsed light source to provide a continuous extreme ultraviolet spectrum, a monochromator to disperse the radiation, an absorption cell, and a photomultiplier to detect the incident and transmitted ultraviolet energy. The photomultiplier output was amplified, detected synchronously at the light source firing rate, and the output recorded on an XY recorder.

The light source was a triggered low-pressure condensed spark in air, employing a uranium anode and a very low-inductance capacitor.[9] Quite high current densities were obtained with this low inductance. This feature,

together with the use of a high atomic-number anode, produced the Vodar continuum[10] from greater than 1000 Å to at least 300 Å.

The radiation was dispersed using a 1-meter Seya-Namioka monochromator with a gold-coated, 1200 line/mm tripartite grating blazed for 750 Å. The linear dispersion at the exit slit was 120μ/Å and the resolution was 0.75 - 1.0 Å. The main chamber of the monochromator was pumped with a four-inch diffusion pump using a liquid nitrogen-cooled trap. With the light source operating at a pressure of 30μ, the main chamber pressure was (1-10) x 10^{-5} Torr, depending on the slit sizes and the pressure in the absorption chamber.

Radiation passing through the exit slit entered the absorption chamber which consisted of a cylinder of length ℓ = 37.0 cm. The gas to be studied was admitted into this cell through a leak valve, and pumped out by the main chamber diffusion pump via the exit slit of the monochromator. All gas pressures in this state of "dynamic equilibrium" were measured with a McCleod gauge attached to the cell. A given pressure of argon could be maintained to 3-4% for an indefinite length of time.

The detector was an ITT FW 131 windowless electron multiplier to which was attached a large copper cathode. The use of the copper photocathode reduced the sensitivity of the detector to bothersome long-wavelength scattered light, and emitted less noise than the combination of a fluorescent screen and photomultiplier sensitive to visible radiation. The electron multiplier was isolated from the absorption cell by a very thin collodion film mounted on a nickel mesh. The film was mounted in the blade of a gate valve, and could be used as a gas seal, or moved out of the optical beam. The transmission of the film in the extreme ultraviolet was of the order of ten to twenty percent. The

small amount of gas which did leak into the detector region was removed by a two-inch diffusion pump, also trapped with a liquid nitrogen-cooled baffle.

Current pulses from the multiplier anode were amplified with a wideband voltage amplifier and fed to a boxcar integrator. The integrator was triggered by the oscillating voltage on the capacitor plates obtained through a capacitive voltage divider. Each time the light source fired, the boxcar integrator would be triggered and an electronic gate would open for a period of about 3μsec. The voltage appearing at the input during this interval was integrated and averaged and the average value recorded on an XY recorder. A typical spectrum of the argon 3s-np autoionizing features is shown in Fig. 2.

RESULTS AND DISCUSSION

We measured the equivalent width of the 3s-4p transition at argon pressures of 0.018 Torr to 0.213 Torr with a constant path length of $\ell = 37.0$ cm. The corresponding observed range of β was 0.72 to 8.52, respectively. The zero light level was determined before, during, and after the measurements, and the pressure was allowed to equilibrate for several minutes at each new pressure. The data are presented in Fig. 3. Each point shown in Fig. 3 is an average of 4-10 scans over the same line.

The experimental error in the measurements is about 8-15% for $\beta > 2$. Several sources of error become important at small values of β and give rise to a spread of about 20% in the measurements with $\beta < 2$. The light source itself has a weak, erratic emission line (due to either air or argon ions in the lamp) which overlaps the lower-energy edge of the argon resonance, and which contributes about 10-15% to the equivalent width at these absorptions.

Another source of error is inherent to the Beutler-Fano shape itself. The wings of the profile extend over many linewidths, so that some part of the equivalent width is always buried in the noise and amplitude fluctuations of the pulsed light source. This latter effect would tend to decrease the value of the equivalent width, and probably compensates in part for the overlapping emission line. Both of these difficulties could be remedied by a source which had low noise, and no emission lines, such as the electron synchrotron.

It can be seen from Eq. (4) that W is a function of the three independent line parameters so that, in principle, it takes only three measurements of W at different β to obtain Γ, $|q|$, and ρ^2. In actual practice, where experimental errors are involved, one must take many more measurements, and then systematically search for the parameters Γ, $|q|$, ρ^2 which give the minimum-error fit to the experimental widths. The analysis which we used to obtain the line parameters was done in the following way: from a preliminary study of the data and the theoretical curves of growth we found that the variation of the equivalent width with β was fairly insensitive to the value of q for the small value of q encountered. For convenience, we started with the value of $|q| = 0.22$ from the work of Madden, Ederer, and Codling.[6] By examining the relative shape of the experimental variation of W with β, and comparing this to the theoretical shape for several values of ρ^2, we determined the best-fit value of ρ^2. Then, having the proper shape, we determined Γ by normalizing the experimental values of W to the theoretical values of W/Γ. We found the parameters for the best fit to be $\rho^2 = 0.85 \pm 0.02$ and $\Gamma = 1.45 \pm 0.29$ Å (0.083 ± 0.017 eV). This compares with the high resolution values[4] of $\rho^2 = 0.86 \pm 0.04$ and $\Gamma = 1.40 \pm 0.09$ Å (0.080 ± 0.005 eV). The

major source of error in our determination of Γ was due to small periodic nonlinearities in the grating sine-bar drive. These were in part minimized by calibrating the linear dispersion with several Ar VII, VI, and V lines excited by running the lamp in argon.

The results of the fit for three values of $\rho^2 = 0.80$, 0.85, and 0.90 are shown in Fig. 3. Also, using the best-fit parameters found above, we have plotted in Fig. 4 the curves of growth for $|q| = 0.0$ and 0.5, along with the curve for $|q| = 0.22$. The three curves all fall fairly close together, but the value of $|q|$ does lie somewhere between 0.0 and 0.5. This situation improves somewhat for larger values of $|q|$ where (see Fig. 1) curves for different $|q|$ lie further apart.

In addition, by measuring $I/I_0 = \exp(-\sigma_t N\ell)$ away from the resonance, we found that the total continuum absorption cross section σ_t was $(33 \pm 2) \times 10^{-18}\,cm^2$, which compares with the values $(35 \pm 2) \times 10^{-18}\,cm^2$ of Ref. 4 and $(33 \pm 2) \times 10^{-18}\,cm^2$ of Ref. 5.

The curve-of-growth approach can be used to obtain values of the line parameters when sufficiently high resolution is not available. Another application of this technique is useful when the line parameters Γ, $|q|$, and ρ^2 are known from previous measurements on a particular line. If we then measure the equivalent width of this line at two different pressures, we can, using the appropriate curve of growth, find the values of β in our experiment. We then have the product $N\ell$, so that knowing either the particle density or the path length, we can determine the other. This approach is useful in, for example, a King furnace or a plasma where one often knows the path length quite accurately, but has no measure of the particle density.

Finally, during the course of this work we learned of a previous study of autoionizing curves of growth by Nossal and Weiss.[11] Our treatment differs from theirs in several ways. We have set up the problem in a universal form which is also easy for experimenters to use. We have also verified experimentally that the autoionizing lines do grow as calculated, and we have attempted to define the limits of usefulness of this technique.

CONCLUSIONS

Curves of growth were derived for lines having the Beutler-Fano form of absorption cross section. The curves were calculated and displayed for $\rho^2 = 1$, and a generating expression given for values of $\rho^2 < 1$. Although a formal curve-of-growth analysis can at best yield only the magnitude of q, the sign may sometimes be evident from the asymmetry in the observed profile.

The technique is applied to the 3s-4p transition in argon. We have fitted the experimental variation of the equivalent width with pressure, with the theoretical curves for different values of the line parameters. We find good agreement between the line parameters obtained in this way with previous high-resolution measurements on the same line, confirming that the profiles do actually grow as calculated.

REFERENCES

1. U. Fano, Phys. Rev. 124, 1866 (1961).

2. U. Fano and J. W. Cooper, Phys. Rev. 137, 1364 (1965).

3. H. Beutler, Z. Phys. 93, 177 (1935).

4. R. P. Madden and K. Codling, Astrophys. J. 141, 364 (1965).

5. M. E. Levy and R. E. Huffman, J. Quant. Spectrosc. Radiat. Transfer 9, 1349 (1969).

6. R. P. Madden, D. L. Ederer, and K. Codling, Phys. Rev. 177, 136 (1969).

7. See, for example, S. S. Penner, Quantitative Molecular Spectroscopy and Gas Emissivities (Addison-Wesley Pub. Co., Inc., Reading, Mass., 1959), Chap. 4.

8. S. D. Conte, Elementary Numerical Analysis (McGraw-Hill Book Co., New York, 1965), p. 138. We are grateful to Mr. Vern Tice of the USC Computing Center for making available to us his integration program.

9. R. W. Carlson, to be published.

10. G. Balloffet, J. Romand, and B. Vodar, Compt. Rend. 252, 4139 (1961); H. Damany, J.-Y. Roncin, and N. Damany-Astoin, Appl. Opt. 5, 297 (1966).

11. R. Nossal and G. H. Weiss, J. Quant. Spectrosc. Radiat. Transfer 8, 763 (1968).

FIGURE CAPTIONS

Figure 1. Curves of growth of spectral lines having the Beutler-Fano profile. The curves are computed with $\rho^2 = 1$. Curves for $\rho^2 < 1$ can be derived from the generating formula given in Eq. (5).

Figure 2. Recording of the 3s-np Rydberg series in argon with a value of β of 6.8. The wavelength scale is approximate. The slit width here is about $2/3\Gamma$, but we can still pick out the steeper side of the 4p member. In this I/I_o spectrum the steeper side faces lower energy, so that q is negative.

Figure 3. Plot of the experimental equivalent widths (open circles) with the best-fit curve having $\rho^2 = 0.85$, and with curves for $\rho^2 = 0.80$ and 0.90. The value of $|q|$ here is 0.22.

Figure 4. Plot of the experimental equivalent widths (open circles) with the best-fit curve having $|q| = 0.22$, and with curves for $|q| = 0.0$ and 0.5. The value of ρ^2 here is 0.85.

Fig. 1

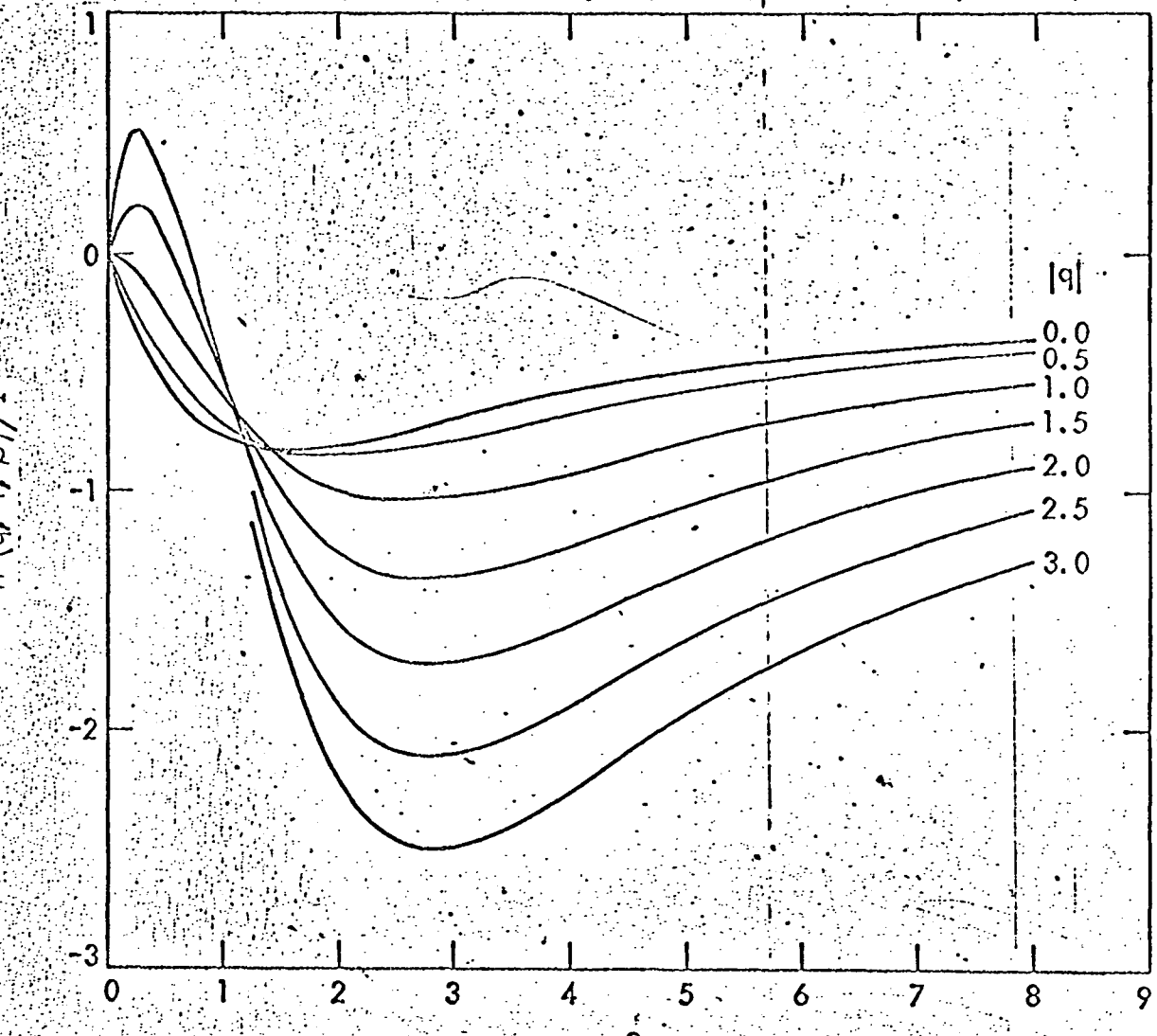

Fig. 2

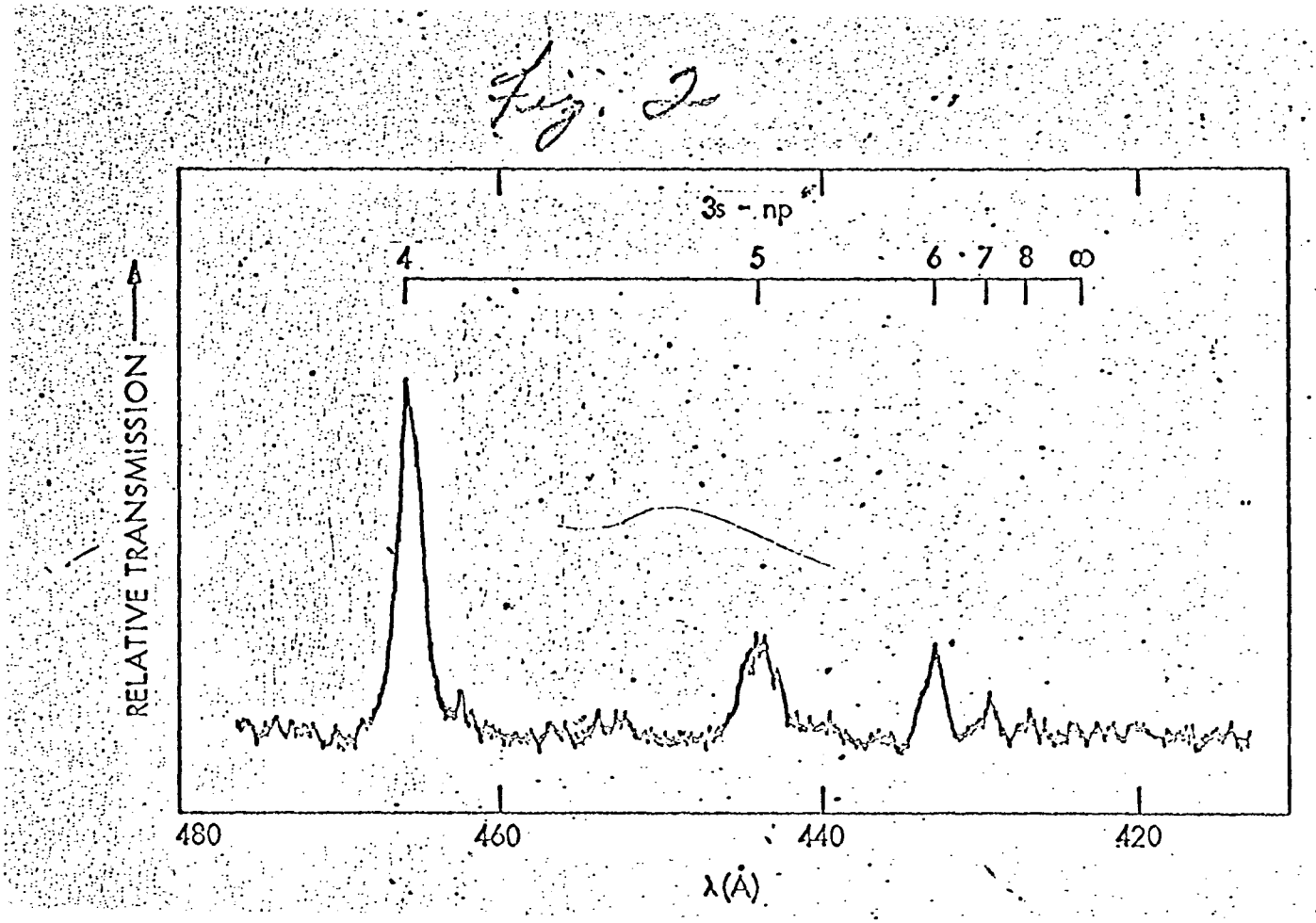

Fig 3

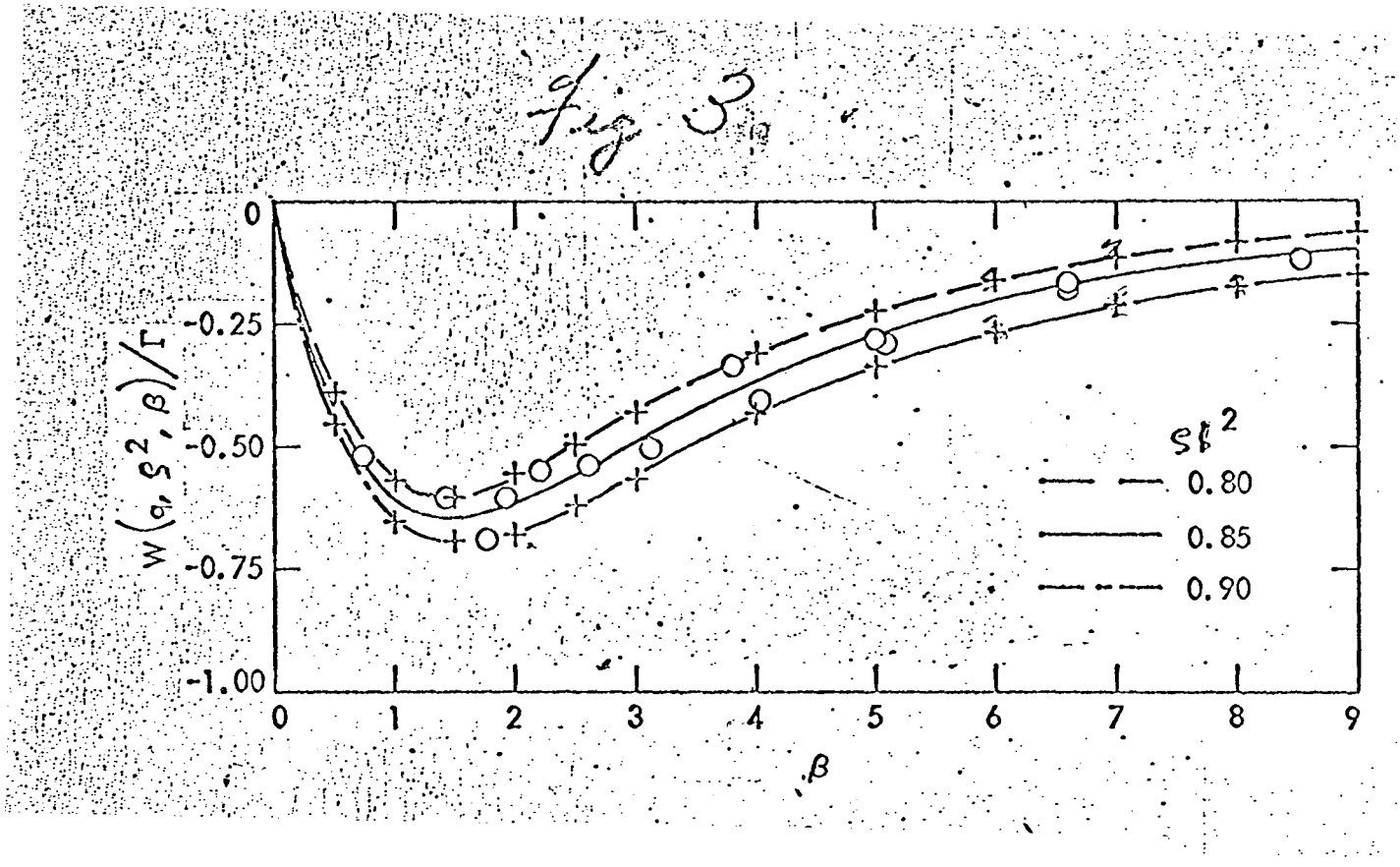

TABLE I. Numerical evaluation of the negative of the integral $W(q,1,\beta)/\Gamma$ from Eq. (4) by Gaussian quadratures. The relative error in the tabulated values is less than 0.035%.

β ↓ / q →	0.0	0.5	1.0	1.5	2.0	2.5	3.0
0.00	0.0000	0.0000	0.0000	0.0000	0.0000	0.0000	0.0000
0.25	0.3261	0.2606	0.0766	-0.1942	-0.5131	-0.8473	-1.1763
0.50	0.5441	0.4599	0.2406	-0.0415	-0.3240	-0.5799	-0.8086
0.75	0.6838	0.6074	0.4272	0.2341	0.0789	-0.0369	-0.1281
1.00	0.7674	0.7121	0.6024	0.5249	0.5034	0.5196	0.5548
1.25	0.8114	0.7824	0.7507	0.7834	0.8768	1.0024	1.1433
1.50	0.8276	0.8254	0.8667	0.9922	1.1763	1.3875	1.6116
1.75	0.8250	0.8474	0.9510	1.1490	1.4008	1.6758	1.9620
2.00	0.8100	0.8535	1.0070	1.2583	1.5580	1.8782	2.2084
2.25	0.7871	0.8477	1.0390	1.3271	1.6588	2.0088	2.3680
2.50	0.7596	0.8335	1.0516	1.3633	1.7142	2.0819	2.4582
2.75	0.7298	0.8135	1.0493	1.3740	1.7344	2.1103	2.4941
3.00	0.6993	0.7897	1.0358	1.3656	1.7282	2.1051	2.4897
3.25	0.6690	0.7637	1.0142	1.3432	1.7026	2.0677	2.4557
3.50	0.6398	0.7366	0.9871	1.3193	1.6636	2.0289	2.4011
3.75	0.6120	0.7093	0.9566	1.2728	1.6157	1.9710	2.3328
4.00	0.5858	0.6824	0.9242	1.2308	1.5625	1.9061	2.2561
4.50	0.5387	0.6313	0.8582	1.1427	1.4501	1.7684	2.0927
5.00	0.4984	0.5853	0.7951	1.0569	1.3399	1.6331	1.9319
5.50	0.4642	0.5448	0.7378	0.9782	1.2384	1.5083	1.7835
6.00	0.4352	0.5096	0.6870	0.9083	1.1483	1.3974	1.6516
6.50	0.4105	0.4792	0.6428	0.8474	1.0697	1.3007	1.5366
7.00	0.3893	0.4529	0.6045	0.7947	1.0018	1.2172	1.4372
7.50	0.3710	0.4301	0.5714	0.7492	0.9432	1.1453	1.3518
8.00	0.3550	0.4103	0.5427	0.7099	0.8927	1.0832	1.2781